



OPEN

## Self-organized wavy infection curve of COVID-19

Takashi Odagaki

Exploiting the SIQR model for COVID-19, I show that the wavy infection curve in Japan is the result of fluctuation of policy on isolation measure imposed by the government and obeyed by citizens. Assuming the infection coefficient be a two-valued function of the number of daily confirmed new cases, I show that when the removal rate of infected individuals is between these two values, the wavy infection curve is self-organized. On the basis of the infection curve, I classify the outbreak of COVID-19 into five types and show that these differences can be related to the relative magnitude of the transmission coefficient and the quarantine rate of infected individuals.

Since November 2019, the pandemic COVID-19 is still expanding in the world. The time dependence of the number of daily confirmed new cases, which I call an infection curve for simplicity, shows clearly a wavy structure in some countries like USA, Japan, Luxembourg and Sweden<sup>1</sup>. Since the period of the wave is much shorter than that of the wave observed in the Spanish flu in 1918–1920, which is believed to be the result of virus mutated while travelling around the globe, there must be a different origin of the wavy infection curve of COVID-19. Besides the wavy infection curve, there are several different types of the infection curve observed in each country in the past 8 months.

Epidemic oscillations have been investigated on the basis of compartmental models<sup>2,3</sup>. Most of approaches attributed the oscillation to a sinusoidal time dependence of parameters of the model. Oscillations in SIR models have also been discussed by evolving networks<sup>4</sup> and asynchronous probabilistic cellular automaton<sup>5</sup>. Recently, Greer et al<sup>6</sup> proposed a simple dynamical model with timevarying births and deaths to explain sustained periodicity of epidemics like smallpox. These approaches may not be appropriate to COVID-19 since (1) there are strong effects of measures including social-distancing on the outbreak, (2) presymptomatic and asymptomatic patients are infectious and (3) these patients can be identified and quarantined by PCR (Polymerase Chain Reaction) test.

The transmission coefficient of the virus from an infected individual to a susceptible individual depends on the trait of the virus as well as the frequency of social contact. Depending on the infection status, a government imposes a strong measure or a moderate request of lockdown and citizens reduce social contact among them voluntarily, which introduces fluctuation of the transmission coefficient.

In this paper, I investigate various infection curves on the basis of SIQR model, focusing on the fluctuation of the transmission coefficient which depends on the infection status. In “[Wavy infection curve in Japan](#)”, I first analyze the wavy infection curve of COVID-19 in Japan and show that it can well be fitted by a transmission coefficient depending on the infection status. In “[Self-organization of wavy infection curve](#)”, I investigate a model society where the transmission coefficient takes two-values depending on the phase of the outbreak and show that if the sum of quarantine and recovery rates is between these two values, a wavy infection curve is self-organized. Analysis of various infection curves in apparent steady states is presented in “[Assessment of measures](#)”, where I classify them into five types which is related to the relative strength of lockdown and quarantine measures. Results are discussed in “[Discussion](#)”.

### Wavy infection curve in Japan

**Model.** In the SIQR model<sup>7–9</sup>, population are separated into four compartments; susceptible individuals, infected individuals at large (will be called infecteds for simplicity), quarantined patients in hospitals or at home who are no longer infectious in the community and recovered (and died) patients. The population in each compartment are denoted by  $S$ ,  $I$ ,  $Q$  and  $R$ , respectively, and the total population is given by  $N (= S + I + Q + R)$ . The basic equations for the time evolution of the populations are given by a set of ordinary differential equations.

$$\frac{dS}{dt} = -\beta_I S \frac{I}{N} \quad (1)$$

<sup>1</sup>Kyushu University, Fukuoka 819-0395, Japan. <sup>2</sup>Research Institute for Science Education, Inc., Kyoto 603-8346, Japan. email: t.odagaki@kb4.so-net.ne.jp

$$\frac{dI}{dt} = \beta_I S \frac{I}{N} - q_I I - \gamma I \quad (2)$$

$$\frac{dQ}{dt} = q_I I - \gamma' Q \quad (3)$$

$$\frac{dR}{dt} = \gamma I + \gamma' Q \quad (4)$$

The term  $\beta_I S \frac{I}{N}$  denotes the net rate at which infections spread, where  $\beta_I$  is a transmission coefficient determined by the characteristics of virus and by lockdown measure, social-distancing and self-isolation of people. Infected individuals at large, regardless of whether they are symptomatic or asymptomatic, are quarantined at a per capita rate  $q_I$  and become non-infectious to the population. Namely, the quarantine rate  $q_I$  is defined by the ratio of the number of quarantined infected-individuals  $\Delta Q(t)$  and the number of infecteds  $I(t)$  at time  $t$ ;  $q_I = \Delta Q(t)/I(t)$ . The quarantine rate is determined by the government policy on PCR test. Quarantined patients recover at a per capita rate  $\gamma'$  (where  $1/\gamma'$  is the average time it takes for recovery) and infected individuals at large become non-infectious at a per capita rate  $\gamma$  (where  $1/\gamma$  is the average time that an infected patient at large is capable of infecting others). It is apparent that Eqs. (1)–(4) guarantee the conservation of population  $N = S + I + Q + R$ .

At the end of November 2020, the total number of infected, quarantined and recovered people is much smaller than the entire population in any countries, and thus the pandemic can be regarded as in its early stage far from the stage of herd immunization. Therefore, I can assume that  $I + Q + R \ll N$  is satisfied and  $S = N - (I + Q + R) \cong N$ . Then the basic equation governing the time evolution of the number of infected is written as

$$\frac{dI}{dt} = \beta_I I - q_I I - \gamma I \equiv \lambda_I I, \quad (5)$$

where the net rate of change of the number of infected is denoted as

$$\lambda_I = \beta_I - q_I - \gamma \quad (6)$$

which determines the short-term behavior of the number of infected. The number of infected increases when  $\lambda_I > 0$  and decreases when  $\lambda_I < 0$ .

It is straightforward to obtain the solution to Eq. (5) in the time period where  $\lambda_I$  does not have apparent dependence on  $I(t)$ :

$$I(t) = I(t_0) \exp \left\{ \int_{t_0}^t \lambda_I(t') dt' \right\}, \quad (7)$$

where  $I(t_0)$  is the initial number of infected at  $t = t_0$ .

### Analysis of the infection curve in Japan

The observed data for the outbreak of COVID-19 is the daily confirmed new cases  $\Delta Q(t)$ , which is given by a convolution of the waiting time distribution function  $\psi(t)$  for quarantining an infected individual and the number of infecteds  $I(t)$ . Therefore  $\Delta Q(t)$  can be expressed as

$$\Delta Q(t) = \int_{-\infty}^t \psi(t-t') I(t') dt'. \quad (8)$$

Since the waiting time distribution function can be assumed to be a well behaved function with a single peak<sup>10,11</sup>, the convolution can be evaluated by the saddle-point method of integration and it is given by<sup>8</sup>

$$\Delta Q(t) = \sqrt{\frac{2\pi}{|\psi''(\tau)|}} \psi(\tau)^{3/2} I(t-\tau), \quad (9)$$

where  $\tau$  is a characteristic time representing the peak position of  $\psi(t)$  and  $\psi''(t) = \frac{d^2\psi(t)}{dt^2}$ . Therefore, in the time period where  $\lambda_I(t)$  does not depend on  $I(t)$ , I can show that

$$\frac{\Delta Q(t)}{\Delta Q(t_0)} = \frac{I(t-\tau)}{I(t_0-\tau)} = \exp \left\{ \int_{t_0-\tau}^{t-\tau} \lambda_I(t') dt' \right\}. \quad (10)$$

Changing the integration variable to  $t'' = t' + \tau$  and defining  $\lambda(t) \equiv \lambda_I(t-\tau)$ , I show that the infection curve is written as

$$\Delta Q(t) = \Delta Q(t_0) \exp \left\{ \int_{t_0}^t \lambda(t'') dt'' \right\}. \quad (11)$$

I also define  $\beta(t) \equiv \beta_I(t-\tau)$  and  $q(t) \equiv q_I(t-\tau)$  and express  $\lambda(t)$  as  $\lambda(t) = \beta(t) - q(t) - \gamma$ .

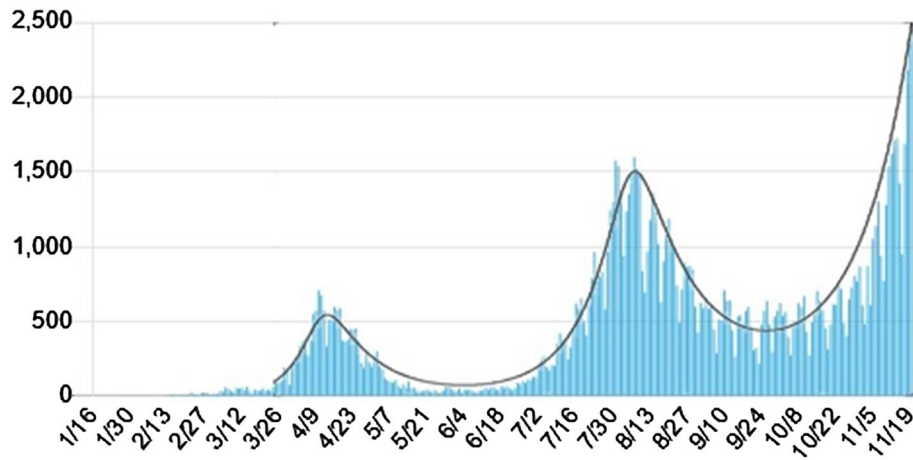


**Figure 1.** The daily confirmed new cases  $\Delta Q(t)$  in Japan from March 26 to November 20, 2020<sup>20</sup>. The solid curve is a fitting by the piece-wise hyperbolic tangent functions for the transmission coefficient with parameters listed in Table 1.

	$t_0$	$t_1$	$t_2$	$t_3$	$t_4$	$t_5$	$t_6$	$t_7$	$t_8$
Date	3/26	4/12	4/30	6/04	7/19	8/03	8/23	10/12	11/21
Days	0	17	35	70	115	130	150	200	240
$\beta_{2i}$	0.18	–	0.007	–	0.138	–	0.04	–	0.127
$dt_{2i+1}$	–	6	–	20	–	6	–	30	–

**Table 1.** Parameters for the fitting in Fig. 1. The quarantine rate is increased from  $q(0) = 0.02$  to  $q(200) = 0.029$  as explained in the text and  $\gamma = 0.04$  is fixed.

The first wave of the outbreak of COVID-19 in various countries has been analyzed on the basis of Eq. (11), where  $\Delta Q(t)$  is approximated by a piece-wise simple exponential function<sup>8,9,12–16</sup>.

In order to fit the infection curve in Japan by Eq. (11), I first assume that  $\gamma$  is a constant since no treatment could be given to infecteds and set  $\gamma = 0.04$ <sup>10,11,17</sup>.

Next, I assume that  $\beta(t)$  and  $q(t)$  change in time continuously between two values represented by a hyperbolic tangent function

$$F(x) = A_{if} \tanh\left(\frac{x - x_m}{dx_m}\right) + B_{if}, \tag{12}$$

which satisfies  $F(x_i) = F_i$  and  $F(x_f) = F_f$  and  $x_i \leq x_m \leq x_f$ , namely

$$A_{if} = \frac{F_i - F_f}{\tanh\left(\frac{x_i - x_m}{dx_m}\right) - \tanh\left(\frac{x_f - x_m}{dx_m}\right)}, \tag{13}$$

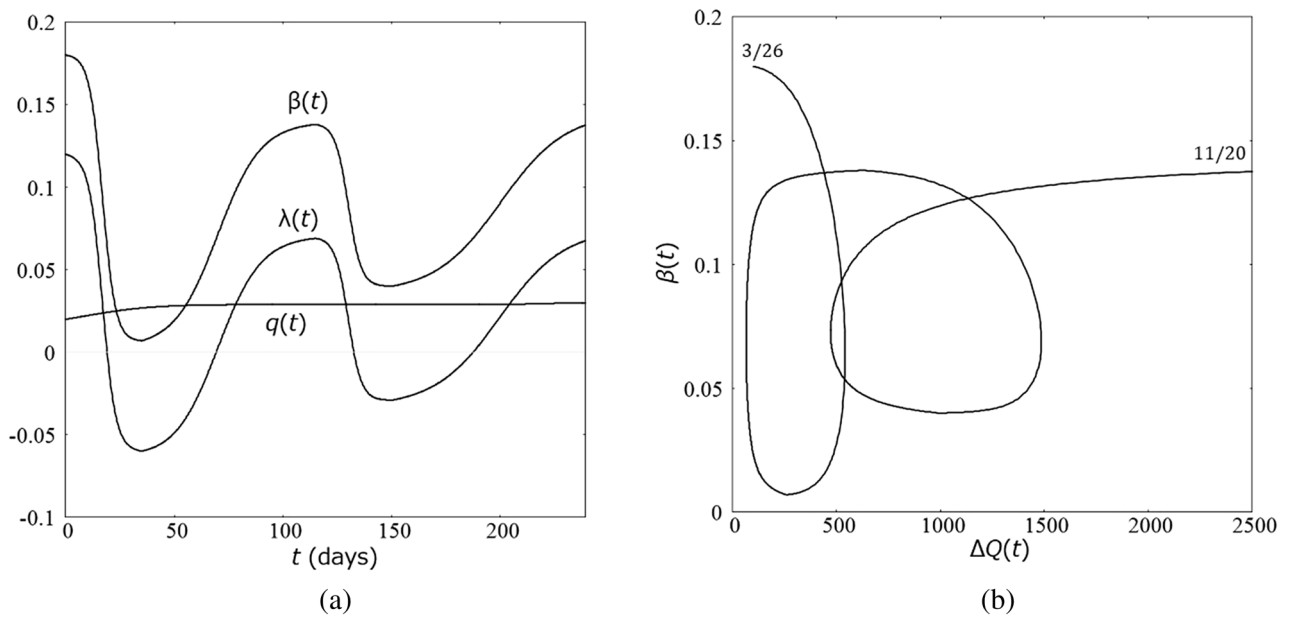
$$B_{if} = F_i - A_{if}. \tag{14}$$

Function  $F(x)$  changes from  $F(x_i) = F_i$  to  $F(x_f) = F_f$  continuously between  $x \sim x_m - dx_m$  and  $x \sim x_m + dx_m$ . The fitting procedure is as follows. First, I assumed that the quarantine rate satisfies  $q(0) = 0.02$  and  $q(200) = 0.029$  and transition occurs at  $t_q = 10$  with width  $dt_q = 30$  as given by Eqs. (12)–(14).

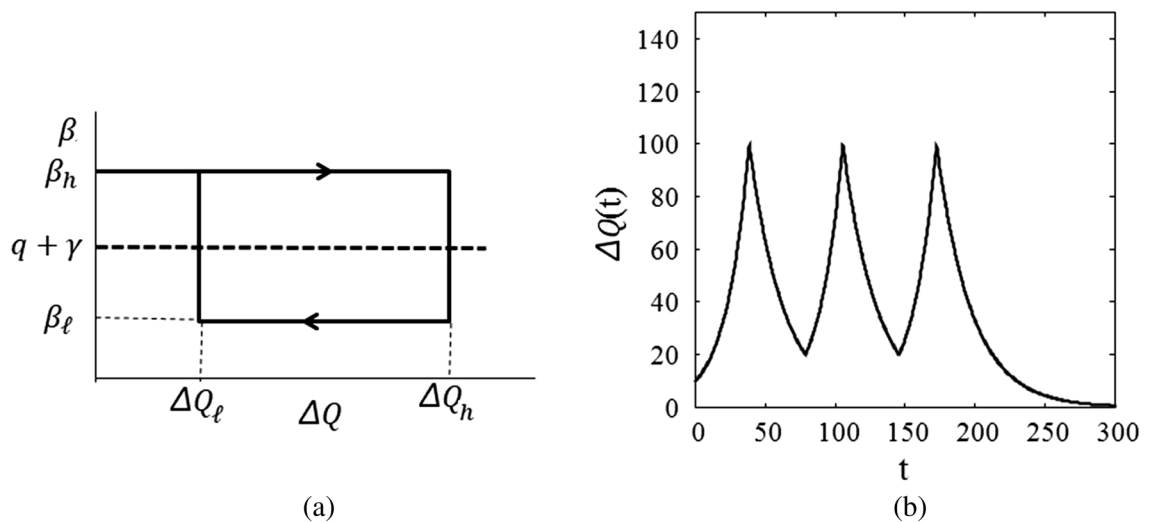
Then, the transmission coefficient is assumed to be given by Eq. (12) for  $t_{2i} \leq t \leq t_{2i+2}$  with  $\beta(t_{2i}) = \beta_{2i}$  and  $\beta(t_{2i+2}) = \beta_{2i+2}$  and  $t_{2i+1}$  as the transition point and  $dt_{2i+1}$  as the width of the transition ( $i = 0, 1, 2, \dots$ ).

Figure 1 shows the daily confirmed new cases in Japan from March 26 (day 0) to November 20 (day 239), 2020. The solid curve in Fig. 1 represents a fitting by piece-wise hyperbolic tangent functions for time-dependent transmission coefficient and quarantine rate with fixed  $\gamma = 0.04$ . Table 1 summarizes parameters determining the time dependence of  $\beta(t)$  used for fitting in Fig. 1.

Figure 2a shows the time dependence of  $\beta(t)$ ,  $q(t)$  and  $\lambda(t)$  and Fig. 2b shows a parametric plot of  $\beta(t)$  as a function of  $\Delta Q(t)$ . It should be emphasized that the assignment of  $\beta$  and  $q$  from  $\lambda$  is not unique since adding any amount to  $\beta$  and  $q$  at a given time does not change  $\lambda$ . In the present study, I assumed that the time dependence of  $q$  is weak since the procedure of the PCR test did show no drastic change in the period for identifying infected individuals at large.



**Figure 2.** (a) Parameters for the transmission coefficient  $\beta(t)$ .  $\beta(t) = A \tanh\left(\frac{t-t_{2i+1}}{dt_{2i+1}}\right) + B$  is set to satisfy  $\beta(t_{2i}) = \beta_{2i}$  and  $\beta(t_{2i+2}) = \beta_{2i+2}$  for  $t_i$ 's listed in Table 1. (b) Parametric plot of  $\beta(t)$ , as a function of  $\Delta Q(t)$  for Japan from March 26 to November 20, 2020.



**Figure 3.** (a) Model transmission coefficient depending on  $\Delta Q$  and  $d\Delta Q(t)/dt$ . (b) Wavy infection curve for the model transmission coefficient.

### Self-organization of wavy infection curve

The time dependence of the transmission coefficient  $\beta(t)$  must be attributed to the attitude of people to self-isolation under government policy and massive information from news media. As Fig. 2b indicates,  $\beta(t)$  has a strong correlation to  $\Delta Q(t)$ . Therefore, I consider the transmission coefficient be a function of  $\Delta Q(t)$  and  $d\Delta Q(t)/dt$ , and I introduce a model country in which  $\beta(t)$  is given by

$$\beta(\Delta Q) = \begin{cases} \beta_h & \text{when } \frac{d\Delta Q}{dt} > 0 \text{ and } \Delta Q \leq \Delta Q_h \\ \beta_\ell & \text{when } \frac{d\Delta Q}{dt} < 0 \text{ and } \Delta Q \geq \Delta Q_\ell \end{cases} \quad (15)$$

where  $\beta_\ell < q + \gamma < \beta_h$  is satisfied. Figure 3a shows  $\beta(\Delta Q)$ . Note that Eq. (11) can still be used in each time period where  $\beta(t)$  is a constant.

The infection curve for  $\beta(\Delta Q)$  given by Eq. (15) is shown in Fig. 3b, where I set  $\Delta Q(0) = \Delta Q_0 = 10$ ,  $\Delta Q_h = 100$  and  $\Delta Q_\ell = 20$ , and  $\beta_h = 0.15$ ,  $\beta_\ell = 0.05$  and  $q = 0.05$ ,  $\gamma = 0.04$ . In this plot,  $\Delta Q_\ell$  is set to 0 after

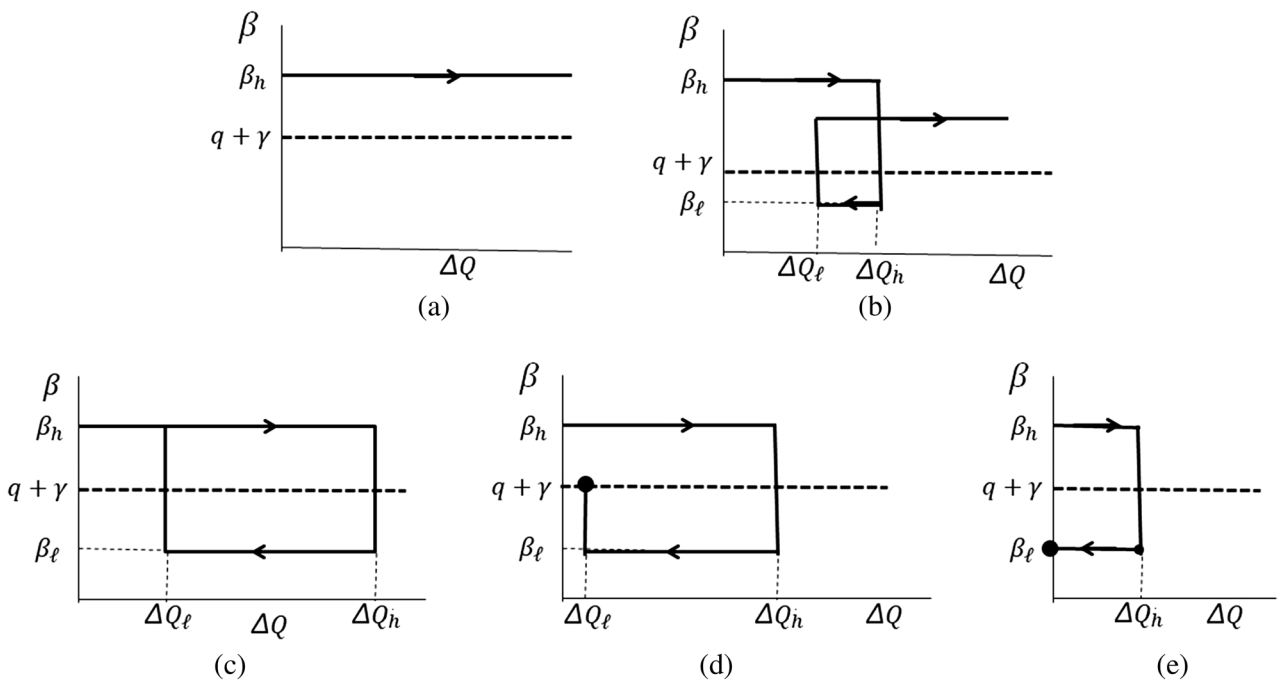


**Figure 4.** Expected relative magnitude of  $\beta(\Delta Q)$  and  $q + \gamma$ , which is shown for fixed  $q + \gamma$ . (a) Type I, (b) Type II, (c) Type III, (d) Type IV and (e) Type V.

the third wave. The infection curve clearly shows wavy nature. If  $\Delta Q_\ell$  is kept at the same value after the third wave, the wavy infection curve continues.

If  $\beta(\Delta Q)$  is given by a continuous function, then the infection curve becomes a smooth function as in Fig. 1.

### Assessment of measures

According to the data available at Coronavirus Resource Center, Johns Hopkins University<sup>1</sup>, the steady behavior of the infection curve in each country up to November 19th seems to be classified into the following five types:

Type I The infection curve keeps increasing, like Jordan, Ukraine and Morocco.

Type II After some number of peaks, the infection curve increases again like Type I. This is seen in Japan, USA, Russia, Canada and many European countries. This can be changed to Type III by some measures.

Type III The infection curve shows oscillation like in UAE, Finland and Ireland. Countries in this type move easily to Type II unless strong measures are introduced to move to Type V.

Type IV Infection curve is characterized by a sharp peak followed by more or less constant infection for a long time. This infection curve is seen in Ecuador, Kuwait and Honduras. Countries in this type usually move to either Type II or Type III, though they could move to Type V.

Type V After a small peak, few new cases are observed like in China, Taiwan, Thailand and Viet Nam.

As discussed in “Analysis of the infection curve in Japan”, the relative magnitude of  $\beta$  and  $q + \gamma$  must be responsible for the structure of the infection curve. Here, keeping  $q + \gamma$  constant, I discuss the relative magnitude of these parameters for different types of infection curve. It should be emphasized that the difference  $\beta - (q + \gamma)$  determines the infection curve. For the sake of simplicity, I fix  $q + \gamma$  and attribute all effects to change in  $\beta$ . It is possible to discuss in the same way by changing  $q$  with a fixed  $\beta$ .

For Type I infection curve,  $\beta > (q + \gamma)$  is satisfied (Fig. 4a) and thus the infection curve keeps increasing. The infection curve will reach eventually its maximum and start to decline because of the non-linear term  $SI/N$  in Eqs. (1) and (2). The Spanish flu belongs to this type.

Type II infection curve will be realized when a strong lockdown measure is introduced at the outbreak and it is lifted in fear of economic break down (Fig. 4b). After a little peak and some length of tail, the infection curve will follow the same trend as Type I.

Wavy infection curve (Type III, Fig. 4c) has already been discussed in “Analysis of the infection curve in Japan”.

Infection curve of Type IV is characterized by a fixed point in the  $\beta - \Delta Q$  plane which is reached after the first peak (Fig. 4d), and  $\Delta Q_\ell$  determines the size of the daily confirmed new cases.

Type V infection curve represents the most efficient measure; the transmission coefficient is brought below  $q + \gamma$  (or  $q$  is increased) so that  $\beta < (q + \gamma)$  is satisfied, and the measure is kept. The trajectory in the  $\beta - \Delta Q$  plane has a fixed point near  $\Delta Q = 0$  as shown in Fig. 4e.

## Discussion

In this paper, I discussed the infection curves of COVID-19 observed in many countries and showed that the infection curve in an apparent steady state can be classified into five types. In particular, a wavy infection curve can be self-organized due to change in self-isolation and/or quarantine measures making  $\beta$  above or below  $q + \gamma$ . It is shown that these different infection curves are caused by relative strength of lockdown measure and quarantine measure. It should be emphasized that the infection curve is determined by the interplay between transmission of the virus and quarantine of patients, and thus unless loosening of lockdown measures is compensated by strengthening of quarantine measures, the infection will continue to expand.

It will be possible to formulate the optimum policy specific to the country for controlling the outbreak on the basis of the present theoretical framework, if the cost function and the aim of policy in each country are given<sup>18</sup>.

The pandemic in countries whose infection curve is of Type I or Type II will stamp out when sufficient number of population get immunized. According to percolation theory<sup>19</sup>, the condition for the herd immunity is that the fraction of immunized individuals is larger than a critical value

$$p_c = 1 - \frac{4.5}{n\beta} \quad (15)$$

where  $\beta$  is the transmission coefficient and  $n$  is the average number of people with whom an infected individual meets while it is infectious. The critical value depends on  $\beta$  and  $n$  and it could be as large as 50–80%. Therefore, it could take much longer time before the herd immunity for COVID-19 is realized in any countries in the world.

Received: 10 October 2020; Accepted: 6 January 2021

Published online: 21 January 2021

## References

1. Coronavirus Resource Center, Johns Hopkins University. <https://coronavirus.jhu.edu/>.
2. Hethcote, H. W. The mathematics of infectious diseases. *SIAM Rev.* **42**, 599–653. <https://doi.org/10.1137/S0036144500371907> (2000).
3. Earn, D. J. D. A light Introduction to modelling recurrent epidemics. in *Mathematical Epidemiology. Lecture Notes in Mathematics*, Vol. 1945 (eds. Brauer, F., van den Driessche, P. & Wu, J.) 3–17 (Springer, Berlin, 2008). <https://doi.org/10.1007/978-3-540-78911-6>.
4. Zhang, X., Shan Jin, C. Z. & Zhu, H. Complex dynamics of epidemic models on adaptive networks. *J. Differ. Equ.* **266**, 803–832. <https://doi.org/10.1016/j.jde.2018.07.054> (2019).
5. Chavez, L. L. & Monteiro, R. H. A. Oscillations in an epidemiological model based on asynchronous probabilistic cellular automaton. *Ecol. Complex.* **31**, 57–63. <https://doi.org/10.1016/j.ecocom.2017.03.001> (2017).
6. Greer, M. *et al.* Emergence of oscillations in a simple epidemic model with demographic data. *R. Soc. Open Sci.* **7**, 191187. <https://doi.org/10.1098/rsos.191187> (2020).
7. Hethcote, H. W., Zhien, M. & Shengbing, L. Effects of quarantine in six endemic models for infectious diseases. *Math. Biosci.* **180**, 141–160 (2002).
8. Odagaki, T. Analysis of the outbreak of COVID-19 in Japan by SIQR model. *Infect. Dis. Model.* **5**, 691–698. <https://doi.org/10.1016/j.idm.2020.08.013> (2020).
9. Suda, R. Report on COVID-19 verification case study in nine countries using the SIQR model. <https://www.medrxiv.org/content/https://doi.org/10.1101/2020.10.07.20208298v1> (2020).
10. Backer, J. A., Klinkenberg, D. & Wallinga, J. Incubation period of 2019 novel coronavirus (2019-nCoV) infections among travellers from Wuhan, China, 20–28 January 2020. *Eurosurveillance* **25**, 2000062. <https://doi.org/10.2807/1560-7917.ES.2020.25.5.2000062> (2020).
11. He, X. *et al.* Temporal dynamics in viral shedding and transmissibility of COVID-19. *Nat. Med.* **26**, 672–675. <https://doi.org/10.1038/s41591-020-0869-5> (2020).
12. Pedersen, M. G., Meneghini, M. Quantifying undetected COVID-19 cases and effects of containment measures in Italy: Predicting phase 2 dynamics. <https://doi.org/10.13140/RG.2.2.11753.85600> (2020).
13. Tiwari, A. Modelling and analysis of COVID-19 epidemic in India. <https://doi.org/10.1101/2020.04.12.20062794> (2020).
14. Tiwari, A. Temporal evolution of COVID-19 in the states of India using SIQR model. <https://doi.org/10.1101/2020.06.08.20125658> (2020).
15. Sedov, L., Krasnochub, A. & Polishchuk, V. Modeling quarantine during epidemics and mass-testing using drones. <https://doi.org/10.1101/2020.04.15.20067025> (2020).
16. Crokidakis, N. COVID-19 spreading in Rio de Janeiro, Brazil: Do the policies of social isolation really work?. *Chaos Solit. Fractals* **136**(109930), 1–6. <https://doi.org/10.1016/j.chaos.2020.109930> (2020).
17. Housen, T., Parry, A. E. & Sheel, M. How long are you infectious when you have coronavirus? *The Conversation*, April 13, 2020 6.20 a.m. AEST. <https://theconversation.com/how-long-are-you-infectious-when-you-have-coronavirus-135295> (2020).
18. Odagaki, T. Exact properties of SIQR model for COVID-19. *Phys. A* **564**, 125564. <https://doi.org/10.1016/j.physa.2020.125564> (2020).
19. Odagaki, T. *The Physics of Connectivity*, 86–87 (Shokabou, Tokyo, 2020).
20. Ministry of Health, Labor, Welfare of Japan. <https://www.mhlw.go.jp/stf/covid-19/kokunainohasseijoukyou.html>.

## Author contributions

T.O. did all the works related to this manuscript.

## Competing interests

The author declares no competing interests.

## Additional information

**Correspondence** and requests for materials should be addressed to T.O.

**Reprints and permissions information** is available at [www.nature.com/reprints](http://www.nature.com/reprints).

**Publisher's note** Springer Nature remains neutral with regard to jurisdictional claims in published maps and institutional affiliations.



**Open Access** This article is licensed under a Creative Commons Attribution 4.0 International License, which permits use, sharing, adaptation, distribution and reproduction in any medium or format, as long as you give appropriate credit to the original author(s) and the source, provide a link to the Creative Commons licence, and indicate if changes were made. The images or other third party material in this article are included in the article's Creative Commons licence, unless indicated otherwise in a credit line to the material. If material is not included in the article's Creative Commons licence and your intended use is not permitted by statutory regulation or exceeds the permitted use, you will need to obtain permission directly from the copyright holder. To view a copy of this licence, visit <http://creativecommons.org/licenses/by/4.0/>.

© The Author(s) 2021